Biomechan Model Mechanobiol (2004) 3: 98–113
DOI 10.1007/s10237-004-0052-9

ORIGINAL PAPER

P. N. Watton · N. A. Hill · M. Heil

A mathematical model for the growth of the abdominal aortic aneurysm

Received: 12 December 2003 / Accepted: 14 July 2004 / Published online: 25 September 2004

Abstract We present the first mathematical model to account for the evolution of the abdominal aortic aneurysm. The artery is modelled as a two-layered, cylindrical membrane using nonlinear elasticity and a physiologically realistic constitutive model. It is subject to a constant systolic pressure and a physiological axial prestretch. The development of the aneurysm is assumed to be a consequence of the remodelling of its material constituents. Microstructural 'recruitment' and fibre density variables for the collagen are introduced into the strain energy density functions. This enables the remodelling of collagen to be addressed as the aneurysm enlarges. An axisymmetric aneurysm, with axisymmetric degradation of elastin and linear differential equations for the remodelling of the fibre variables, is simulated numerically. Using physiologically determined parameters to model the abdominal aorta and realistic remodelling rates for its constituents, the predicted dilations of the aneurysm are consistent with those observed in vivo. An asymmetric aneurysm with spinal contact is also modelled, and the stress distributions are consistent with previous studies.

1 Introduction

This paper is concerned with the modelling of the abdominal aortic aneurysm (AAA), which is characterised by a bulge in the abdominal aorta. Development of the AAA is associated with a weakening and dilation of the arterial wall and the possibility of rupture; 80–90% of ruptured aneurysms will result in death (Wilmink et al. 1999). Surgery to remove the aneurysm is an option, but it is a high-risk procedure with a 5% mortality rate (Raghavan and Vorp 2000). The aims of mathematical modelling of aneurysms are to lead to a greater understanding of the pathogenesis of the disease and improved criteria for the prediction of rupture.

The evolution of an aneurysm is assumed to be a consequence of the remodelling of the artery's material constituents. The microstructural characteristics of the artery need to be incorporated into the model so that tissue remodelling can be addressed. The abdominal aorta is a large artery of elastic type (Holzapfel et al. 2000; Humphrey 1995). It consists of three layers, the intima, media and adventitia. The intima is the innermost layer, the adventitia the outermost. The media is sandwiched between these two layers and is separated from them by the internal elastic lamellae, which are thin elastic sheets composed of elastin. A substantial part of the arterial wall volume consists of an intricate network of macromolecules consitituting the extra-ceullular matrix (e.c.m.). This matrix is composed of a variety of versatile proteins that are secreted locally, by fibroblast cells, and assembled into an organized meshwork in close association with the surface of the cell that created them. The e.c.m. determines the tissue's structural properties. For an artery it consists primarily of elastin, collagen, smooth muscle and ground substance; a hydrophilic gel within which the collagen and elastin tissues are embedded. Elastin and collagen are the main load bearers. Collagen is the stiffer and most nonlinear of the two materials, but at low strains elastin bears most of the load. This is because at physiological strains the collagen is tortuous in nature, and is crimped in the unstrained artery (Shadwick 1999; Raghavan et al. 1999). The elastin gives rise to the artery's isotropic and rubber-like behaviour for small deformations whereas the collagen gives rise to the anisotropy and high

P. N. Watton (✉)
Department of Cardiac Surgery,
University of Glasgow, Royal Infirmary,
10 Alexandra Parade, Glasgow, G31 2ER, UK
E-mail: P.Watton@clinmed.gla.ac.uk
Tel.: +44-141-2227863

N. A. Hill
Department of Mathematics,
University of Glasgow, University Gardens,
Glasgow, G12 8QW, UK

M. Heil
Department of Mathematics,
University of Manchester, Oxford Road,
Manchester, M13 9PL, UK

nonlinearity at larger deformations. For modelling purposes, the mechanical contribution from the smooth muscle is ignored (Holzapfel et al. 2000). Dilation of an aneurysm is accompanied by a loss of elastin and a weakening of the arterial wall (He and Roach 1993). As the wall dilates, strains in the elastin and collagen increase. Elastin is a stable protein with a long half-life (Alberts et. al. 1994), whereas collagen is in a continual state of deposition and degradation (Humphrey 1999) with a considerably faster turnover. The highly nonlinear tensile nature of the collagen implies that collagen remodelling is necessary to account for the large dilations observed in aneurysms. Without remodelling, even if all the elastin degraded, the strains in the collagen, and thus the dilation of the wall, would not have to increase significantly for the total load to be borne.

The remodelling of arteries in response to changes in their external environment is a recognised phenomenon and has been considered by, for example, Fung et al. (1993), Rachev and Meister (1998) and Rodriguez et al. (1994). However, their analyses were phenomenologically based, the remodelling driven, for example, by changes in the thickness, opening angle or compliance of the arterial wall, rather than explicitly associated with adaptations of its microstructural architecture. More recently, Humphrey (1999) has proposed a microstructurally based model which addresses the remodelling of collagen in altered configurations and considers the simple case of remodelling at extended and contracted lengths for a uniaxial model in which the fibres attach with zero strain. This idea is employed in this work; however, here it is assumed that the collagen fibre attaches and configures itself such that its strain at systole is a constant, $\varepsilon_a > 0$. This remodelling process may be advantageous for the artery because it adapts so that the load is primarily borne by the elastin during the cardiac cycle, and the collagen adapts such that it acts only to prevent large strains occurring in the arterial wall.

The abdominal aorta is modelled as a cylindrical tube subject to an axial pre-stretch and a constant internal systolic pressure. The distal and proximal ends of the abdominal aorta are fixed to simulate vascular tethering by the renal and iliac arteries. The constitutive equations proposed by Holzapfel et al. (2000) to model the arterial wall are developed to include microstructural features of the structure of the collagen, namely fibre recruitment and density variables; these enable the remodelling of collagen to be simulated. The development of aneurysm is modelled as the deformation that arises as the material constituents of the artery remodel whilst it is subject to a constant pressure. Where possible we have based parameter values on those from the literature, however, some may be coarsely estimated/assumed and further experimental research is required to accurately determine values.

The systolic blood pressure is 16 KPa whilst the peak wall shear stress is 2.5 Pa (Cheng et al. 2002), thus mechanically the shear stress has a negligible effect on the deformation. However, the permeability of the intima is dependent on the magnitude of the shear stress (Lever 1995). As the aneurysm develops, the dynamics of the fluid flow will change. Consequently, the magnitudes of the shear stress exerted on the intima, and the permeability of the intima will change. The permeability of the intima may play an important role in the biochemical processes that lead to the destruction of the elastin, thus the fluid mechanics may be an important aspect of aneurysm development. However, there is little data on the temporal and spatial degradation of elastin, let alone the physiological processes linking this to the uptake of substances from the bloodstream. Consequently, we have decided to ignore the fluid dynamical effects and simply prescribe the degradation of elastin.

As the aneurysm develops in size, the naturally occurring process of fibre turnover acts to restore the strain in the fibres. This is desirable mechanical behaviour as it shifts the load bearing back to the more compliant elastin. In our model, we introduce recruitment variables, which define the factors by which the tissue must be stretched with respect to the undeformed configuration, for the collagen to begin to bear load. This allows us to simulate the gross mechanical effects of fibre turnover in altered configurations. As the material constituents remodel, the new equilibrium displacement field for the arterial wall needs to be calculated. The wall is treated as a membrane and so a variational equation over a two-dimensional domain governs the ensuing deformation and evolution of the aneurysm. A finite element method is employed to solve the resulting equations. We obtain realistic rates of dilation for physiologically realistic geometric, material and remodelling parameters. Dilation rates are seen to increase in hypertensive conditions. To further test the consistency of our model we compare the predicted stress distributions with those predicted by previous mathematical models of developed aneurysms.

2 The recruitment variable

An integral part of this work is defining recruitment variables, which define the factors by which the tissue must be stretched, for the collagen fibres to bear load. This enables key aspects of the naturally occurring physiological process of collagen fibre deposition and degradation in the altered configuration to be modelled. Consider a specimen of homogeneous arterial tissue, with the collagen fibres arranged parallel along its length (Fig. 1a). If the tissue is stretched parallel to the axis of

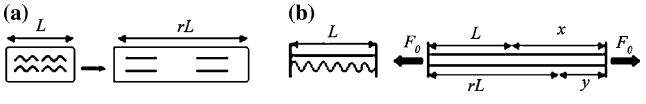

Fig. 1 **a** Collagen fibres are recruited, i.e. begin to bear load, when unstrained tissue is stretched by a factor r. **b** The uni-axial model. In the unstrained state, the collagen is crimped and the length of elastin is L. A *constant force* is applied to both ends. In the initial equilibrium state the strain in the collagen is ε_a

the collagen fibres, then beyond a critical stretch, the fibres will be *recruited*, and begin to bear load. The factor the tissue must be stretched for this to occur is defined by the recruitment variable r. In fact, at the microscopic level, the fibres are distributed with a range of waviness (Armeniades et al. 1973) and here r relates to those fibres that are recruited first. Once recruitment begins, the collagen bears a load and the subsequent mechanical behaviour of the whole population of fibres can be modelled (Armentano et al. 1991).

The strain in the collagen is defined with respect to the configuration in which it is recruited, whilst the strain in the elastin is always defined with respect to the initial reference configuration. Consider Fig. 1b, which depicts a parallel arrangement of elastin and collagen. The length L denotes the length of the unstrained tissue and x its extension. In unstrained tissue, the strain in the elastin is taken to be zero, and thus the strain in the elastin is measured with respect to the undeformed configuration. The Green's strain in the elastin is

$$\varepsilon_{\mathrm{E}} = \frac{((L+x)/L)^2 - 1}{2}. \tag{1}$$

Collagen fibres are recruited when the unstrained tissue is stretched by a factor r. Hence, the strain in the collagen, ε_{C}, is defined with respect to onset of collagen recruitment, i.e.

$$\varepsilon_{\mathrm{C}} = \frac{[(rL+y)/rL]^2 - 1}{2}, \quad y = L + x - rL. \tag{2}$$

Combining Eqs. 1 and 2 gives

$$\varepsilon_{\mathrm{C}} = \frac{\varepsilon_{\mathrm{E}} + (1-r^2)/2}{r^2}. \tag{3}$$

The significance of this relationship, i.e. Eq. 3, is that r can remodel to maintain the strain in the collagen to some equilibrium value, whilst the strain in the elastin increases as the aneurysm dilates.

To model the deformations that occur as the elastin degrades and collagen remodels, it is necessary to define an equilibrium level of strain for the fibres, which the collagen attempts to maintain by remodelling. However, the choice of this equilibrium strain is not straightforward. In the physiological range of strains, collagen contributes partly to the load bearing of the arterial wall. As strains in the arterial wall increase, collagen becomes the main load bearer and, due to its highly nonlinear mechanical behaviour, quickly prevents strains becoming excessive. Consequently, to account for the large dilations observed in aneurysms, remodelling of collagen must be occurring. Thus, it is hypothesized: collagen remodels to maintain an equilibrium level of strain in its fibres.

This is consistent with the fact that collagen fibres are in a continual state of degradation and deposition (Humphrey 1999), and that the fibres attach in a state of strain (Alberts et al. 1994). In this work, the equilibrium strain, ε_{a}, is defined to be the strain in the collagen at systole. The justification for this definition of ε_{a} is based on the following reasoning.

- The fibroblasts work on the collagen they have secreted, crawling over it and tugging on it—helping to compact it into sheets and draw it out into cables, i.e. they act to attach the collagen fibres to the e.c.m in a state of strain (Alberts et al. 1994, p 984). Therefore, it may be hypothesized that there is a maximum attachment strain that the fibroblasts can achieve.
- We assume that the time taken for the fibroblasts to configure the collagen fibres is much longer than the duration of a pulse, so that the maximum fibre attachment strain will occur at the systolic (peak) strain of the cardiac cycle. This implies the peak strain in the fibres is equal to the peak attachment strain.
- Fibres that achieve maximum attachment strains are the first to be recruited as the tissue is strained. Thus the definition of a maximum attachment strain is consistent with the definition of r, which relates to those fibres that are recruited first. Other fibres with lower levels of attachment strain are recruited at a later stage, which is accounted for by the proposed stress functions to model the gross mechanical behaviour of the population of collagen fibres.

Note, not all fibres attach with the maximum attachment strain. There would be a distribution of attachment strains achieved; this is consistent with the variability in waviness of a population of collagen fibres. In this work, we assume that the recruitment distribution function is unchanged throughout the remodelling. This is unlikely, as changes in the distribution of the population of collagen fibres may occur, and could be an important aspect of the remodelling. However, this would lead to added complexity, and at this stage, more insight may be gained with a simpler model—so here we assume that the mechanical behaviour of a population of collagen fibres is fixed throughout the remodelling. However, such features could be included in later developments.

If collagen is recruited when the tissue has been stretched by a factor r, and if a systolic stretch is achieved when tissue has been stretched by a factor λ_{s}, then from Eq. 3 the attachment strain is

$$\varepsilon_{\mathrm{a}} = \frac{\lambda_{\mathrm{s}}^2 - r^2}{2r^2}. \tag{4}$$

Other definitions may be proposed for this parameter. Further experimental work is needed to clarify the nature of the attachment of collagen fibres in altered configurations as the aneurysm develops, and test the validity of these assumptions.

We now consider a conceptual one-dimensional model to gain insight into the mechanical aspects of the remodelling. Consider Fig. 1b, which illustrates a parallel arrangement of elastin and collagen, subject to a *constant force* F_0. The force balance equation is

$$A_{\mathrm{E}}(t)\sigma_{\mathrm{E}}(\varepsilon_{\mathrm{E}}) + A_{\mathrm{C}}(t)\sigma_{\mathrm{C}}(\varepsilon_{\mathrm{C}}) - F_0 = 0, \tag{5}$$

where A_E (t) and $A_C(t)$ represent cross-sectional areas, and $\sigma_E(\varepsilon_E)$ and $\sigma_C(\varepsilon_C)$ the Piola–Kirchhoff stresses for the elastin (E) and collagen (C), respectively. Initially, the system $(t=0)$ is assumed to be in equilibrium, and thus the strain in the collagen is ε_a. If the elastin degrades then, since a fixed axial force is acting, the system will stretch and the strain in the collagen will increase so that $\varepsilon_C > \varepsilon_a$. If the strain in the collagen deviates from the equilibrium strain, it is hypothesized that a remodelling process acts to restore the strain to ε_a. If it is assumed that the population distribution of fibres remains the same, then for the collagen to restore its strain to ε_a, two processes can occur:

- The recruitment variable r can increase in value until a new equilibrium configuration is achieved.
- The collagen can thicken. This will act to contract the uniaxial system and restore the strain in the collagen. This is achieved by remodelling the cross-sectional area, $A_C(t)$, of collagen. An increase in $A_C(t)$ is consistent with the fact that an increase in the collagen content is observed in aneurysms (He and Roach 1993). This may be seen as a desirable remodelling response to the development of the aneurysm for it limits the rate, and extent of the dilation. In this work we attribute the thickening of the collagen to an increase in the density of collagen fibres whilst the dimensions of individual fibres remain the same. However, it may be that it is the number of fibres that remain constant and thicker fibres are laid down. Experimental work is needed to clarify this matter so that more suitable remodelling mechanisms can be proposed.

The remodelling of the recruitment variable is subtle and it is helpful to consider its mechanical effects, in a conceptual one-dimensional model before analysing the more complex geometry of an aneurysm. When elastin degrades, the system will stretch, an increased load will be borne by the collagen, and the compliance will decrease. If the collagen fibres are in a continual state of deposition and degradation then this turnover will cause the tissue to stretch yet further until a new equilibrium is restored. This will shift some of the load-bearing back to the elastin and reduce the load borne by the collagen, and the strain of the fibres, thus increasing the compliance. Figure 2 considers the effects of fibre deposition and degradation, on the scale of the collagen fibres, for a tissue that is stretched and held at fixed length whilst remodelling occurs, and illustrates that this physiological process can be simulated by remodelling the recruitment variable r.

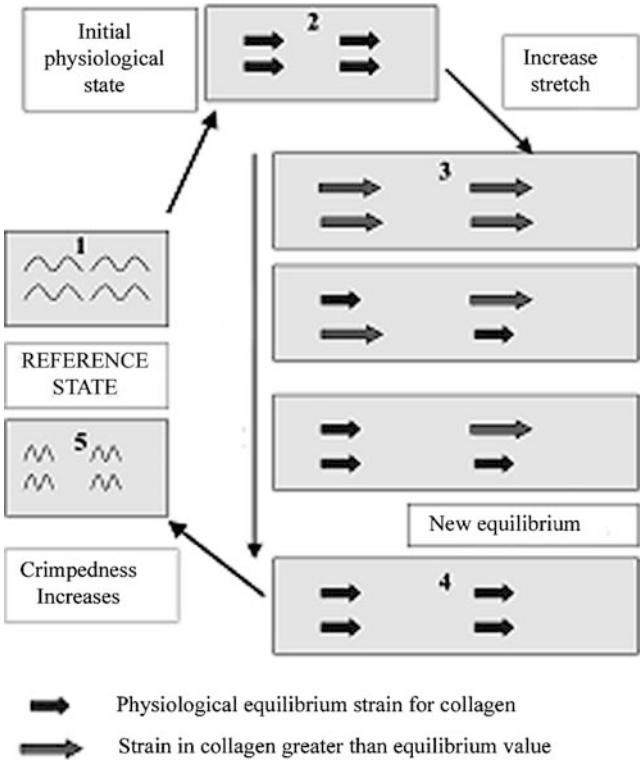

Fig. 2 Attachment of collagen fibres in altered configurations. **1** The reference state is the original undeformed configuration of the tissue. In the undeformed state, the fibres have a characteristic waviness. **2** The initial physiological state is such that the strain in the collagen fibres is the equilibrium value. At systole, the strain in the fibres is ε_a. The tissue is currently in equilibrium. Although the fibres are in a continual state of degradation and deposition, new fibres will attach with identical levels of strain to those that decay and thus no changes occur in the mechanical properties of the tissue. **3** Suppose the tissue is stretched further and, for the purposes of this example, held at fixed length. New fibres attach to the tissue so that at the new systolic configuration their strain is ε_a. The old fibres decay, and the distribution of collagen fibres changes. The naturally occurring turnover of the fibres, will proceed to restore strain in all the fibres to equilibrium levels. **4** All of the old fibres have decayed and have been replaced by new fibres of strain ε_a. The artery reaches a new equilibrium configuration. **5** If the tissue is contracted back to the reference configuration, the crimp of the collagen will have increased. Equivalently, the factor the tissue must be stretched for the collagen to be recruited has increased. Hence the effects of deposition and degradation in altered configurations can be captured by remodelling the recruitment variable r—which relates to the waviness of collagen in the undeformed configuration

3 Mathematical description of the deformation

The strain field through the thickness of the normal arterial wall is approximately uniform about the physiological range of strains (Fung and Choung 1986). If it is assumed that the mechanism by which collagen fibres attach to the artery, is independent of the current configuration of the artery, then this process may naturally maintain a uniform strain field (in the collagen) throughout the thickness of the arterial wall as the aneurysm develops. The deformations at a constant systolic pressure are considered. Thus for the purposes of studying the deformations that arise as the aneurysm develops it is sufficient to consider only the strains in the midplane, and this is the approach we adopt; we have modelled the arterial wall as a membrane, using a geometric nonlinear membrane theory (see e.g. Wempner 1973; Heil 1996).

In general, a body-fitted coordinate system is used to describe the membrane with Lagrangian coordinates x^α ($\alpha = 1, 2$) parallel to the midplane and the x^3 coordinate perpendicular to it. The midplane is positioned at $x^3 = 0$; the upper and lower surfaces of the membrane have coordinates $x^3 = \pm h/2$, where h is the thickness of the membrane. Lower case letters refer to the undeformed reference state, upper case to the deformed state. The Einstein summation convention is used throughout. The position of a material point on the midplane of the membrane is given by $\mathbf{q}\ (x^1, x^2, x^3 = 0) = \mathbf{q}^0\ (x^1, x^2)$. The covariant base vectors, which are tangent to the coordinate lines, x^α, on the midplane, are given by

$$\mathbf{a}_\alpha = \frac{\partial \mathbf{q}^0}{\partial x^\alpha} = \mathbf{q}^0_{,\alpha}, \tag{6}$$

where the comma denotes partial differentiation with respect to x^α . The unit normal to the two midplane base vectors is chosen as the third midplane base vector, i.e.

$$\mathbf{a}_3 = \frac{\mathbf{a}_1 \wedge \mathbf{a}_2}{|\mathbf{a}_1 \wedge \mathbf{a}_2|}. \tag{7}$$

The covariant midplane metric tensors in the undeformed configuration are $a_{ij} = \mathbf{a}_i \cdot \mathbf{a}_j$. During the deformation a material point on the membrane's midplane, which was at a position $= \mathbf{q}^0\ (x^\alpha)$, in the undeformed reference configuration, is displaced to a new position

$$\mathbf{Q}^0(x^\alpha) = \mathbf{q}^0(x^\alpha) + \mathbf{v}(x^\alpha), \tag{8}$$

where $\mathbf{v}(x^\alpha)$ is the midplane displacement field. The tangent vectors to the deformed midplane are thus

$$\mathbf{A}_\alpha = \mathbf{Q}^0_{,\alpha} = \mathbf{a}_\alpha + \mathbf{v}_{,\alpha}. \tag{9}$$

The normal to the midplane base vectors, $\mathbf{A}_3$, is chosen as the third midplane base vector, with the magnitude defined such that the incompressibility condition is satisfied on the midplane, i.e.

$$\mathbf{A}_3 = \frac{(\mathbf{A}_1 \wedge \mathbf{A}_2)|\mathbf{a}_1 \wedge \mathbf{a}_2|}{|\mathbf{A}_1 \wedge \mathbf{A}_2|}. \tag{10}$$

The covariant midplane metric tensors in the deformed configuration are $A_{ij} = \mathbf{A}_i \cdot \mathbf{A}_j$ ($i, j = 1, 2, 3$). If it is assumed that off-midplane strain field is equal to that of the midplane then the Green's strain tensor can be expressed in terms of the difference of the midplane metrics,

$$\varepsilon_{ij} = \frac{A_{ij} - a_{ij}}{2}. \tag{11}$$

We now turn to the specific geometry of our model of the aneurysm. The abdominal aorta is modelled as a thin cylinder of undeformed radius R, length L, and thickness h. The thicknesses of the media and adventitia are denoted h_M and h_A respectively. It is subject to a physiological axial pre-stretch, ${\lambda_z}^0$, and a constant systolic pressure p_0 (= 16 kPa) which causes a circumferential stretch of λ_θ^0. The initial in vivo configuration is thus a cylindrical tube of length ${\lambda_z}^0 L$, radius ${\lambda_\theta}^0 R$, and thickness $h/{\lambda_z}^0{\lambda_\theta}^0$. The ends of the initial deformed configuration are fixed throughout the deformation to simulate vascular tethering by the renal and iliac arteries. The cylindrical polar Lagrangian coordinates, x^i ($i = 1,2,3$), denote arc lengths in the axial, azimuthal and radial directions, respectively. The vector to a material point on the midplane before the deformation is thus

$$\mathbf{q}^0 = \left[R \sin\left(\frac{x^2}{R}\right), R\cos\left(\frac{x^2}{R}\right), x^1\right] \quad \text{for } x^1 \in [0, L],\ x^2 \in [0, 2\pi R). \tag{12}$$

After the deformation, the material point on the midplane is displaced to a new position,

$$\mathbf{Q}^0 = [(R + v^3)\sin\,\theta + v^2\cos\,\theta, (R + v^3)\cos\,\theta - v^2 \sin\,\theta, x^1 + v^1], \tag{13}$$

where $\theta = x^2/R$, and v^1, v^2, v^3 denote the displacements in the axial, azimuthal and radial directions, respectively. The strain field for the midplane is calculated using Eqs. 6, 7, 8, 9, 10 and 11.

4 Governing equations

The principle of virtual displacements,

$$\delta\Pi_\mathrm{strain} - \delta\Pi_\mathrm{load} = 0, \tag{14}$$

governs the deformation, where $\delta\Pi_\mathrm{strain}$ is the variation of the strain energy stored in the deformed aneurysm wall and $\delta\Pi_\mathrm{load}$ is the work done by the pressure, p, acting on the tube surface during a virtual displacement, i.e.

$$\int_v \delta w\, dv - \oint_S p(\hat{\mathbf{A}}_3 \cdot \delta\mathbf{Q}^0) dS = 0, \tag{15}$$

where $\delta\mathbf{Q}^0 = \delta(\mathbf{q}^0 + \mathbf{v}) = \delta v^i \mathbf{a}_i$, $dS = |\mathbf{A}_1 \wedge \mathbf{A}_2|\ dx^1\ dx^2$, and $\hat{\mathbf{A}}_3 = (\mathbf{A}_1 \wedge \mathbf{A}_2)/|\mathbf{A}_1 \wedge \mathbf{A}_2|$. Here, we make the approximation that the virtual displacement of the upper and lower surfaces is equal to that of the midplane and that the area elements of the upper and lower surfaces are equal to that of the midplane. The assumption that the strain field in the aneurysm tissue is uniform through the thickness of the arterial wall, i.e. the strain field of the off-midplane is equal to that of the midplane, implies that the strain energy density functions (SEDFs), w, are independent of x^3 . This enables an immediate integration yielding

$$\int_0^{2\pi R}\int_0^L [\delta(h_\mathrm{M} w_\mathrm{M} + h_\mathrm{A} w_\mathrm{A}) - p(\mathbf{A}_1 \wedge \mathbf{A}_2) \cdot \delta v^i \mathbf{a}_i]\, dx^1\, dx^2 = 0. \tag{16}$$

Appropriate functional forms for the SEDFs for the media, w_M, and adventitia, w_A, are required.

5 Strain energy density functions for aneurysmal tissue

The aneurysm develops as the material constituents remodel; thus it is important to use a constitutive model that accounts for the microstructure of the artery. Holzapfel et al. (2000) have recently proposed a general constitutive model that explicitly accounts for the individual contributions of the elastin and the collagen in the arterial wall. It is assumed that the mechanical response of the artery is due to the media and the adventitia, i.e. the intima is not considered to contribute mechanically. Each layer is modelled as a fibre reinforced composite. The structure of the collagen was determined experimentally. It was found that the fibres are arranged in double helical structures of pitches $\pm\gamma_{\mathrm{M}}$ in the media and of pitches $\pm\gamma_{\mathrm{A}}$ in the adventitia. The SEDF is split into two parts, one for isotropic properties and the other for anisotropic properties. It is supposed that the mechanical response of the artery at low strains is governed by the non-collagenous constituents (elastin) that respond isotropically. The mechanical response at high strains is governed chiefly by the collagenous constituents that are anisotropic. A classical neo-Hookean model is used to model the isotropic response in each layer. An exponential functional form was used to describe the energy stored in the collagen fibres, so that the strong stiffening effect that occurs at high pressures could be captured. Holzapfel et al. (2000) propose SEDFs for the media, w_{M}, and adventitia, w_{A}, given by

$$w_{\mathrm{M}} = c_{\mathrm{M}}(\varepsilon_{11}+\varepsilon_{22}+\varepsilon_{33}) + \sum_{\varepsilon^2_{\mathrm{M_p}}\geq 0,\mathrm{p}=\pm} k_{\mathrm{M}}\left(\exp\left[a_x\varepsilon^2_{\mathrm{M_p}}\right]-1\right), \tag{17}$$

$$w_{\mathrm{A}} = c_{\mathrm{A}}(\varepsilon_{11}+\varepsilon_{22}+\varepsilon_{33}) + \sum_{\varepsilon^2_{\mathrm{A_p}}\geq 0,\mathrm{p}=\pm} k_{\mathrm{A}}\left(\exp\left[a_x\varepsilon^2_{\mathrm{A_p}}\right]-1\right), \tag{18}$$

where

$$\varepsilon_{J_{\mathrm{p}}} = \varepsilon_{11}\sin^2\gamma_{J_{\mathrm{p}}} + \varepsilon_{22}\cos^2\gamma_{J_{\mathrm{p}}} + 2\varepsilon_{12}\sin\gamma_{J_{\mathrm{p}}}\cos\gamma_{J_{\mathrm{p}}}, \tag{19}$$

is the Green's strain resolved in the direction of a collagen fibre which has an orientation of $\gamma_{J_{\mathrm{p}}}$ to the azimuthal axis. The subscript J takes values M and A, referring to the media and adventitia respectively, and p denotes the pitch $\pm\gamma_J$. For a more complete description of this constitutive model see Holzapfel et al. (2000). Note, Holzapfel et al. (2000) express (17) and (18) in terms of the invariants of the deformation and we have written them explicitly in terms of the Green's strain. The constants c_{M} and c_{A} are associated with the non-collagenous matrix of the material, and a_x, k_{M} and k_{A} with the collagenous part. Previous studies (Holzapfel 2000) have found that the neo-Hookean elastic properties of the adventitia are an order of magnitude lower than that for the media (6–14 times depending on location) and thus they set $c_{\mathrm{A}} = c_{\mathrm{M}}/10$. Holzapfel determined specific parameters for the carotid artery of a rat and hence the actual values of the material parameters are not of relevance here. Note, the fibres are assumed to have no compressive resistance, i.e. the contribution to the strain energy is zero if the fibres are in compression.

These SEDFs can be adapted to include microstructural features for the collagen and elastin. To model aneurysm development we need to prescribe a degradation of elastin. However, little is known other than the initial and final concentrations of elastin (MacSweeney et al. 1992) and thus appropriate assumptions need to be made. The fact that the dilation of the aorta is localized to a specific region would suggest that elastin is being lost principally in a confined region. Here, the concentration of elastin in the arterial wall $c_{\mathrm{E}}(x^1, x^2, t)$ is taken to be a double Gaussian exponential

$$c_{\mathrm{E}}(x^1,x^2,t) = 1-\left(1-(c_{\min})^{t/T}\right) \times \exp\left[-m_1\left(\frac{L_1-2x_1}{L_1}\right)^2 - m_2\left(\frac{L_2-2x_2}{L_2}\right)^2\right], \tag{20}$$

where L_1 and L_2 denote the Lagrangian lengths of the membrane in the axial and circumferential directions, m_1 (>0) and m_2 (>0) are parameters that control the degree of localization of the degradation, and $c_{\min}$ is the minimum concentration of elastin at time $t = T$. This gives a point of minimum concentration of elastin, and the elastin concentration tends towards normal values towards the distal and proximal ends of the abdominal aorta. The timescale of aneurysm development may vary from person to person. Given that average growth rate is 0.4 cm/year (Humphrey 1995), and the decision whether to operate on an aneurysm occurs when the diameter reaches 5–6 cm, then the timescale of development is of the order of 10 years. Estimates for the concentration of elastin in the developed aneurysm suggest that between 63 and 92% of the elastin is lost (He and Roach 1993). We choose $T = 10$ years and $c_{\min} = 0.1$. The spatial degradation is unknown and further experimental work is needed to clarify the distributions before more accurate mathematical models can be proposed. For an axisymmetric degradation Eq. 20 reduces to

$$c_{\mathrm{E}}(x^1,t) = 1-\left(1-(c_{\min})^{t/T}\right)\exp\left[-m_1\left(\frac{L_1-2x_1}{L_1}\right)^2\right]. \tag{21}$$

The SEDF is then the product of the concentration of elastin within the tissue and the neo-Hookean SEDF for the elastin, i.e.

$$w_{\mathrm{elastin}} = k_{\mathrm{E}}c_{\mathrm{E}}(x^1,x^2,t)(\varepsilon_{11}+\varepsilon_{22}+\varepsilon_{33}), \tag{22}$$

where k_{E} is a material parameter to be determined that represents the mechanical behaviour of elastin for the healthy abdominal aorta.

Although the geometry is now more complex, recruitment variables for the collagen fibres can be introduced throughout the tissue. The Green's strains in the collagen, $\varepsilon^{\mathrm{C}}_{J_{\mathrm{p}}}$, are related to the Green's strains of the elastin resolved in the directions of the collagen fibres, $\varepsilon_{J_{\mathrm{p}}}$, via the recruitment variables $r_{J_{\mathrm{p}}}(x^1, x^2, t)$:

$$\varepsilon^{\mathrm{C}}_{J_{\mathrm{p}}} = \frac{\left(\varepsilon_{J_{\mathrm{p}}} + \left(1 - r^2_{J_{\mathrm{p}}}\right)\Big/2\right)}{r^2_{J_{\mathrm{p}}}}, \tag{23}$$

where $r_{J_{\mathrm{p}}}$ defines the factor by which the tissue must be stretched, in the direction of a fibre, with respect to the undeformed configuration, for the collagen fibre to begin to bear a load, and $\varepsilon_{J_{\mathrm{p}}}$ is given by (19). Note again, the subscript J takes values M and A, referring to the media and adventitia respectively, and p denotes the pitch $\pm\gamma_J$. The initial values for recruitment variables, $r^0_{J_{\mathrm{p}}}$, are chosen so that the fibres in the media and adventitia have strains equal to ε_{a} at systole, i.e. collagen fibres in the adventitia have strains identical to those in the media at the systolic pressure at $t=0$, i.e. from Eq. 23

$$r^2_{J_{\mathrm{p}}} = \frac{1 + 2\varepsilon_{J_{\mathrm{p}}}(\lambda_\theta, \lambda_z)}{1 + 2\varepsilon_{\mathrm{a}}}, \tag{24}$$

where the strain in the elastin resolved in the direction of the collagen fibres, $\varepsilon_{J_{\mathrm{p}}}$, is calculated with Eq. 19. A value for ε_{a} now needs to be proposed; experiments to determine its value precisely would be desirable. The media has collagen fibres orientated primarily in the azimuthal direction and is roughly twice the thickness of the adventitia (Table 1). Consequently, the media is the predominant load bearer during radial inflation. Using the pressure–radius graph for a human abdominal aorta given in Lanne et al. (1992) and subtracting the "estimated" contribution from elastin gives an estimate for the circumferential strain, $\lambda_\theta{}^{\mathrm{rec}}$, at which the medial collagen begins to be recruited. This has been achieved quite crudely and more precise experiments would be desirable. Now Eq. 23 implies,

$$r^2_{\mathrm{M_p}} = \frac{1 + 2\varepsilon_{\mathrm{M_p}}}{1 + 2\varepsilon^{\mathrm{C}}_{\mathrm{M_p}}}. \tag{25}$$

At the onset of recruitment the strain in the medial collagen fibres is zero, i.e. $\varepsilon^{\mathrm{C}}_{\mathrm{M_p}} = 0$. The Green's strains are

$$\varepsilon_{11} = \frac{\left(\lambda^0_z\right)^2 - 1}{2}, \quad \varepsilon_{22} = \frac{\left(\lambda^{\mathrm{rec}}_\theta\right)^2 - 1}{2}, \quad \varepsilon_{12} = 0, \tag{26}$$

and so the value of the recruitment variable for the medial collagen at $t = 0\left(r^0_{\mathrm{M_p}}\right)$ is given by Eq. (25) as

$$r^0_{\mathrm{M_p}} = \sqrt{\left(\lambda^0_z\right)^2 \sin^2\gamma_{\mathrm{M}} + \left(\lambda^{\mathrm{rec}}_\theta\right)^2 \cos\gamma_{\mathrm{M}}}, \tag{27}$$

where $\varepsilon_{\mathrm{M_p}}\left(\lambda^0_z, \lambda^{\mathrm{rec}}_\theta\right)$ is calculated using Eq. 19. The collagen fibre attachment strain, ε_{a}, is defined to be the strain in the fibres at the systolic pressure, ($\lambda_\theta = \lambda_\theta{}^0$, $\lambda_z = \lambda_z{}^0$), and thus from Eq. 23,

$$\varepsilon_{\mathrm{a}} = \frac{\varepsilon_{\mathrm{M_p}}\left(\lambda^0_\theta, \lambda^0_z\right) + \left(1 - \left(r^0_{\mathrm{M_p}}\right)^2\right)\Big/2}{\left(r^0_{\mathrm{M_p}}\right)^2}. \tag{28}$$

The initial values for recruitment variable for the adventitia, $r^0_{\mathrm{A_p}}$, are chosen so that the fibres in the adventitia have strains equal to ε_{a} at systole, i.e. collagen fibres in the adventitia have strains identical to those in the media at the systolic pressure at $t=0$. Thus Eq. (24) implies that

$$r^0_{\mathrm{A_p}} = \sqrt{(1 + 2\varepsilon_{\mathrm{A_p}}(\lambda^0_\theta, \lambda^0_z))/(1 + 2\varepsilon_{\mathrm{a}})}. \tag{29}$$

where the strain in the elastin resolved in the direction of the adventitial collagen fibres, $\varepsilon_{\mathrm{A_p}}(\lambda^0_\theta, \lambda^0_z)$, is calculated with Eq. (19).

Table 1 Material constants and physiological data used for modelling the human abdominal aorta

Wall thickness	
Media (h_{M})	1.33 mm
Adventitia (h_{A})	0.67 mm
Collagen fibre angles	
Media (γ_{M})	8.4°
Adventitia (γ_{A})	41.9°
Systolic pressure (p_0)	120 mmHg
Undeformed radius (R)	6.6 mm
Axial pre-stretch ($\lambda_z{}^0$)	1.5
Circumferential stretch	
At onset of recruitment ($\lambda_\theta{}^{\mathrm{rec}}$)	15.2/13.2
At systole ($\lambda_\theta{}^0$)	17.2/13.2
At 200 mmHg ($\lambda_\theta{}^{200}$)	18.5/13.2
Material parameters	
Exponential constant for collagen (a_x)	40
Elastin (k_{E})	97.6 kPa
Ground substance (k_{g})	9.76 kPa
Collagen media (k_{M})	3.52 kPa
Collagen adventitia (k_{A})	0.88 kPa

This data is estimated and determined from the pressure radius curve for the abdominal aorta in Lanne et al. (1992)

6 Strain energy density function for heterogeneous aneurysmal tissue

A normalized density variable is introduced, which defines the density of the collagen fibres with respect to the undeformed configuration of the tissue. The recruitment variables and normalized fibre density variables are incorporated into the strain energy representation for the collagen in Holpzapfel et al.'s (2000) model. Note we assume that the neo-Hookean response in the media has an elastinous and a non-elastinous part, k_{g}, due to the ground substance. Furthermore, we assume that the contribution from the ground substance is equal in the media and adventitia. Note that in Holzapfel et al.'s (2000) model, since there is no degradation of elastin, only one material parameter is required for the

neo-Hookean contribution in the media. The SEDFs, w_J, are thus

$$w_{\mathrm{M}} = (k_{\mathrm{g}} + c_{\mathrm{E}}(x^1, x^2, t)k_{\mathrm{E}})(\varepsilon_{11} + \varepsilon_{22} + \varepsilon_{33}) + \sum_{\varepsilon^{\mathrm{C}}_{\mathrm{M_p}} \geq 0, \mathrm{p}=\pm} r_{\mathrm{M_p}}(x^1, x^2) n_{\mathrm{M_p}}(x^1, x^2) k_{\mathrm{M}} \times \left(\exp\left[a_x \left(\varepsilon^{\mathrm{C}}_{\mathrm{M_p}}\left(\varepsilon_{\mathrm{M_p}}, r_{\mathrm{M_p}}\right)\right)^2 \right] - 1 \right) \quad (30)$$

for $x^3 \in [(-h)/2, (-h + 2h_{\mathrm{M}})/2]$, and

$$w_{\mathrm{A}} = k_{\mathrm{g}}(\varepsilon_{11} + \varepsilon_{22} + \varepsilon_{33}) + \sum_{\varepsilon^{\mathrm{C}}_{\mathrm{A_p}} \geq 0, \mathrm{p}=\pm} r_{\mathrm{A_p}}(x^1, x^2) n_{\mathrm{A_p}}(x^1, x^2) k_{\mathrm{A}} \times \left(\exp\left[a_x \left(\varepsilon^{\mathrm{C}}_{\mathrm{A_p}}\left(\varepsilon_{\mathrm{A_p}}, r_{\mathrm{A_p}}\right)\right)^2 \right] - 1 \right) \quad (31)$$

for $x^3 \in ((h - 2h_{\mathrm{A}})/2, h/2]$. Recall that h_{M}, h_{A}, h ($=h_{\mathrm{M}} + h_{\mathrm{A}}$) denote the thicknesses of the media, adventitia and arterial wall respectively, and $c_{\mathrm{E}}(x^1, x^2, t)$ represents the concentration of elastin in media. $\varepsilon^{\mathrm{C}}_{J_{\mathrm{p}}}(x^1, x^2, t)$ denotes the Green's strain, and $r_{J_{\mathrm{p}}}(x^1, x^2, t)$ and $n_{J_{\mathrm{p}}}(x^1, x^2, t)$, the recruitment and density variables of the collagen fibres, of pitch p in layer J. At $t = 0$, $c_{\mathrm{E}}(x^1, x^2, 0) = n_{\mathrm{M}}(x^1, x^2, 0) = n_{\mathrm{A}}(x^1, x^2, 0) = 1$. Following Holzapfel et al. (2000) we set k_{g} to be an order of magnitude lower than the contribution from the elastin, i.e. $k_{\mathrm{g}} = k_{\mathrm{E}}/10$. Due to a lack of available data on the human abdominal aorta, we have based some of the remaining parameters on those determined by Holzapfel et al. (2000) for the carotid rat artery, namely the fibre angles in the media and adventitia, and the relative magnitude of k_{M}, k_{A}; here we choose $k_{\mathrm{A}} = k_{\mathrm{M}}/4$. This is questionable; experimental work is needed to correctly determine these values. The undetermined constants, k_{E}, k_{M} and a_x, are set so that the strain energy functions model the mechanical behaviour of the abdominal aorta using physiological data (Lanne et al. 1992). Note, the contributions to the strain energy from the collagen fibres arise only when the fibre strains are positive, $\varepsilon^{C}_{J_{\mathrm{p}}} > 0$, i.e. fibres do not contribute to the strain energy when in compression. This SEDF enables remodelling in altered configurations to be addressed. In all, four recruitment variables and four fibre density variables are required. In the absence of physiological data, linear differential equations are proposed for the remodelling of the recruitment and density variables:

$$\frac{\partial r_{J_{\mathrm{p}}}}{\partial t} = \alpha\left(\varepsilon^{\mathrm{C}}_{J_{\mathrm{p}}} - \varepsilon_a\right), \quad \frac{\partial n_{J_{\mathrm{p}}}}{\partial t} = \beta\left(\varepsilon^{\mathrm{C}}_{J_{\mathrm{p}}} - \varepsilon_a\right), \quad (32)$$

where the constants α, $\beta > 0$. The remodelling parameter α was determined to correspond to a prescribed turnover rate of the collagen fibres, as follows. The abdominal aorta is modelled using a physiologically determined set of material parameters and is initially subject to physiological axial and systolic circumferential stretches. The circumferential stretch is then instantaneously increased. The strains in the collagen fibres increase to $\varepsilon^{\mathrm{S}}{}_J$ ($> \varepsilon_{\mathrm{a}}$), and the artery is held in this altered configuration whilst the collagen remodels to restore its strain ε_{a}. Two remodelling mechanisms are considered for restoring strain:

1. A half-life model (Humphrey 1999) which models the mechanical effects of fibres being deposited in the altered configuration with strain ε_{a} and the decay of the strained fibres (with strain $\varepsilon^{\mathrm{S}}{}_J$).
2. Remodelling via the recruitment variable. The kinetics and mechanical effects of the two remodelling mechanisms are compared to give a value for α associated with the turnover rate of the collagen fibres.

It is important to remember that the strain in the elastin is defined with respect to the undeformed configuration, whereas the strain in the collagen is defined with respect to an altered configuration, via the recruitment variable. The recruitment variable remodels to maintain the strain in the collagen to ε_{a}. This is to simulate the effect of fibres being degraded and deposited in altered configurations. It is not regarded as the effect of disattachment and reattachment of fibres, which may occur if the tissue is stretched over much shorter time periods. The fibre density, n_J, is defined with respect to the undeformed configuration of the tissue, and gives an interpretation of the relative density of the fibres as the tissue remodels. If n_J stays constant whilst the recruitment variable remodels then one can picture this as the number of fibres in the arterial wall remaining constant. This allows for a structural interpretation of the remodelled tissue and may be used to predict changes in mass content of collagen. This may be useful, since the mass content of collagen could be measured. Although this may be less easy to determine than the thickness of the tissue, it may yield a better understanding of the structural changes in the tissue. More complex models may be proposed in the future as knowledge of the changing structure of the collagen in the developing aneurysms improves. Ideally the degradation and deposition of the entire population of collagen fibres would be modelled; however, such an approach would be computationally expensive in a full 3D model and it would seem preferable to use variables which are gross mechanical descriptors.

7 Numerical solution

Equation 16 can be written as

$$\int_0^{2\pi R_0} \int_0^{L} \left[(\varphi_i - p_i)\delta v^i + \varphi_{i\alpha}\delta v^i_{,\alpha} \right] dx^1\, dx^2 = 0, \quad (33)$$

where $\varphi_i = \partial(h_{\mathrm{M}} w_{\mathrm{M}} + h_{\mathrm{A}} w_{\mathrm{A}})/\partial v^i$, $\varphi_{i\alpha} = \partial(h_{\mathrm{M}} w_{\mathrm{M}} + h_{\mathrm{A}} w_{\mathrm{A}})/\partial v^i_{,\alpha}$ and $p_i = p(\mathbf{A}_1 \wedge \mathbf{A}_2) \cdot \mathbf{a}_i$ for $i = 1, 2, 3$ and $\alpha = 1, 2$. This equation is solved by applying a displacement-based finite element technique. The displacements are approximated by an ansatz

$$v^i(x^\alpha) = \sum_{g=1}^{N} V^{ig}\psi_g(x^\alpha) \tag{34}$$

for N basis functions, ψ_g; piecewise bilinear shape functions are employed to approximate the displacement field. Similarly, the remodelling variables r_{J_p}, n_{J_p} are defined at nodal points of the domain, with the variables $R^g_{J_p}$ and $N^g_{J_p}$, and interpolated using the shape functions:

$$r_{J_p}(x^\alpha) = \sum_{g=1}^{N} R^g_{J_p}\psi_g(x^\alpha), \quad n_{J_p}(x^\alpha) = \sum_{g=1}^{N} N^g_{J_p}\psi_g(x^\alpha) \tag{35}$$

Now

$$\delta v^i(x^\alpha) = \sum_{g=1}^{N} \delta V^{ig}\psi_g(x^\alpha), \quad \delta v^i_{,\alpha}(x^\alpha) = \sum_{g=1}^{N} \delta V^{ig}\psi_{g,\alpha}(x^\alpha) \tag{36}$$

and so insertion of Eq. (35) into Eq. (32) yields

$$f_{ig} = \sum_{g=1}^{N} \int_0^{2\pi R_0} \int_0^{L} [(\varphi_i - p_i)\psi_g + \varphi_{i\alpha}\psi_{g,\alpha}]\delta V^{ig} dx^1 dx^2 = 0, \tag{37}$$

where $\varphi_i = \varphi_i(c_E(x^1, x^2, t), \quad r_{J_p}(R^g_{J_p}, \psi_g), \; n_{J_p}(N^g_{J_p}, \psi_g), \; v^i(V^{ig}, \psi_g), v^i_{,\alpha}(V^{ig}, \psi_{g,\alpha}))$, with a similar expression for $\phi_{i,\alpha}$. Equation 37 must hold for all variations δV^{ig}. If n_{BC} of the boundary conditions are specified then this equation yields $3N$-n_{BC} equations for the $3N$-n_{BC} unknowns. It is solved using a Newton–Raphson scheme, using the displacement variables as the independent variables. The initial values of the nodal values of the recruitment are given by Eqs. 27 and 29. The nodal values of the fibre density are set equal to 1 throughout the domain. At each time step the remodelling variables are updated with a forward Euler time-integration scheme applied to Eqs. 32, i.e.

$$\begin{aligned} R^g_J(t_{n+1}) &= R^g_J(t_n) + \alpha(\varepsilon^{Cg}_{J_p}(t_n) - \varepsilon_a)\delta t, \\ N^g_J(t_{n+1}) &= N^g_J(t_n) + \alpha(\varepsilon^{Cg}_{J_p}(t_n) - \varepsilon_a)\delta t, \end{aligned} \tag{38}$$

where the nodal value of the strain in the collagen $\varepsilon^{Cg}_{J_p}$ is taken to be the average of the strains in the surrounding elements. The degradation of the elastin is the driving force for the remodelling, it causes the strains in the aneurysm to increase and then the recruitment and density variables remodel to restore the strain in the collagen (with respect to the configuration it is recruited in). A timestep of 0.04 years was employed; decreasing the timestep further made negligible difference to the results and merely increased computational time. The asymmetric model (see below) employed a domain size of 200×50 elements, and the axisymmetric model, 200 line elements. Increasing the number of elements further has a negligible effect on the results (Watton).

Partial integration of Eq. 33 yields $\varphi_i - \varphi_{i\alpha,\alpha} = 0$. The initial displacement field for the artery subject to a pressure p axial stretch λ_z and radial stretch λ_θ with undeformed radius R is $v^1 = (\lambda_z - 1)x^1$, $v^2 = 0$, $v^3 = (\lambda_\theta - 1)R$. This displacement field can be shown to imply that ϕ_i- $\phi_{i\alpha,\alpha} = 0$ ($i = 1, 2, 3$ and $\alpha = 1, 2$) and $\phi_1 = 0$, $\phi_2 = 0$. Thus $\phi_3 = 0$, which implies that

$$p = \frac{1}{R\lambda_z}\left(\underbrace{\left(\underbrace{(h_M + h_A)k_g}_{(1)} + \underbrace{h_M c_E k_E\left(1 - \frac{1}{\lambda_z^2\lambda_\theta^4}\right)}_{(2)}\right)}_{} + \underbrace{\sum_{\substack{J=M,A,\\ \varepsilon^C_{J_p}\geq 0}} \frac{2n_J h_J k_J a_x \varepsilon^C_{J_p} \exp\left[a_x(\varepsilon^C_{J_p})^2\right] \cos^2\gamma_{J_p}}{r^2_{J_p}}}_{(3)}\right). \tag{39}$$

The first term (1) is a contribution from the non-elastinous neo-Hookean constituents in the media and adventitia, the second term (2) arises due to the contribution from the elastin in the media, and the third contribution (3) is due to the collagen in the media and the adventitia. For an artery subject to a physiological axial pre-stretch ($\lambda_z = \lambda_z^0$), the onset of collagen recruitment is estimated to begin at $\lambda_\theta = \lambda_\theta^{rec}$. This enables values for r_M, r_A, ε_a to be determined using the analysis detailed earlier. For a healthy artery $n_J(x^1, x^2, 0) = 1$, and thus in Eq. 39 there are three unknowns to be determined, namely k_E, k_M, a_x (given that $k_A = k_M/4$). It is assumed that at the initial systolic pressure ($\lambda_z = \lambda_z^0$, $\lambda_\theta = \lambda_\theta^0$, $p = p_0$) the neo-Hookean constituents bear 80% of the load. This enables k_E to be determined using Eq. 39, i.e.

$$k_E = R\lambda_{z_0} P^0_{E:C} p_0\left(\frac{h}{10} + h_M\right)\left(1 - \left(\frac{1}{(\lambda_z^0)^2(\lambda_\theta^0)^4}\right)\right) \tag{40}$$

where $P_{E:C}{}^0 = 0.8$ (and $h = h_M + h_A$, $k_g = k_E/10$). At a pressure of 200 mmHg the circumferential stretch, λ_θ^{200}, is determined from Lanne et al. (1992). The proportion of load borne by the elastin, $P_{E:C}{}^{200}$, and collagen ($1 - P_{E:C}{}^{200}$) are found at this increased pressure using Eq. 39. Consequently, there are two equations for the proportion of load borne by the collagen, at the systolic pressure and a pressure of 200 mmHg, which allows the constants a_x and k_M to be determined to achieve the appropriate mechanical nonlinear behaviour for the collagen. Table 1 details the material parameters used in the model, and Fig. 3, the resulting pressure–diameter relationship.

8 Example of an axisymmetric aneurysm

We will now consider the development of an aneurysm that arises due to an axisymmetric degradation of

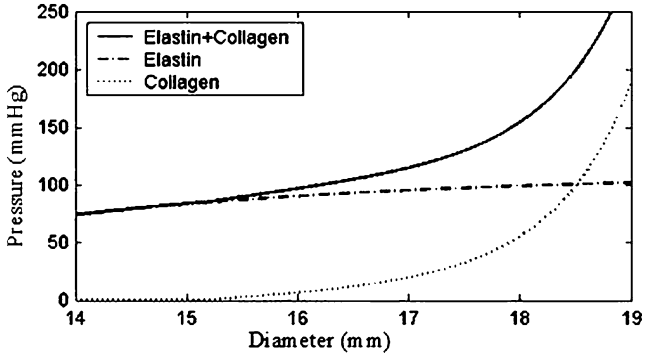

Fig. 3 The pressure–diameter relationship for the model of the abdominal aorta. Here the relationship is shown for an in vivo physiological axial stretch of $\lambda_z = 1.5$

elastin. The degradation of elastin is given by Eq. 21 with $m_1 = 20$ (see Fig. 4a). Appropriate remodeling rate parameters need to be specified for Eqs. 32. Given a value for the remodelling parameter α that corresponds to a physiologically realistic turnover rate of the collagen fibres, the remodelling constant β is then determined so that the aneurysm dilation is physically realistic, i.e. by a factor of 2–3 over a period of 10 years. Humphrey (1999) suggested collagen turnover rates, i.e. the time for 50% of the fibres to decay and be replaced, of 3–90 days, although acknowledging that the timescales may be longer. It was found that correspondings values of α resulted in a very nonlinear remodelling profile, with little dilation initially followed by rapid dilation in the final few years (Watton 2002). Although aneurysms can suddenly expand, the average rate of dilation is 0.4 cm/year (Humphrey 1995) and dilation rates are in the range of 0.3 to 1.1 cm/year (Humphrey 2002). Thus, it was considered physiologically more consistent to choose $\alpha = 12$ ($130 < \beta < 150$), which corresponds to a (longer) half-life of 180 days. This yields an increasing rate of dilation but in a less nonlinear manner (Fig. 5a). It would be desirable if turnover rates of collagen fibres in aneurysms were more precisely known to both improve and validate our modelling.

Fig. 4 **a** Concentration of elastin as a function of the Lagrangian coordinate x^1 for aneurysm in Fig. 5c. **b** Concentration profile as plotted against a spatially fixed Eulerian axial coordinate. t denotes time in years. The Eulerian profile occupies a wider region than the Lagrangian profile due to the axial distortion as the aneurysm develops

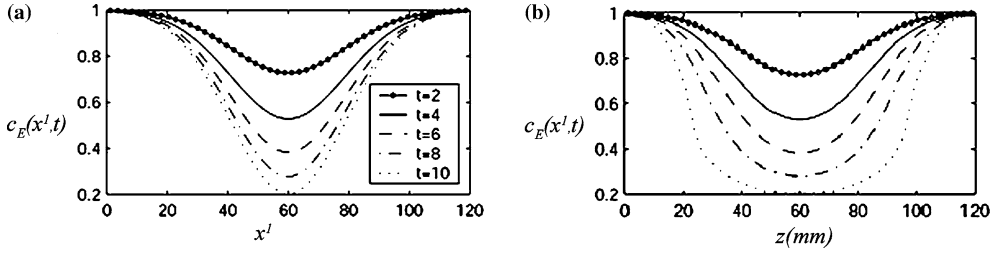

An unusual feature of aneurysm growth is highlighted in the axisymmetric model (Fig. 5c). Large axial deformations occur in addition to the visually apparent, radial deformations. This is a consequence of the fact that, under in vivo normotensive conditions, the abdominal aorta is subject to a large axial stretch. As the elastin degrades, the central region of the aneurysm dilates axially, while the distal and proximal end regions of the aorta retract. As the end regions of the aneurysm retract, the collagen remodels about the new state, which promotes further retraction. Conversely, as the central region dilates axially, the collagen remodels about this new configuration, allowing further axial dilation. This effect is highlighted by the difference in the profiles of the elastin degradation as defined in Lagrangian coordinates (Fig. 4a) and in a spatially fixed Eulerian frame (Fig. 4b). Physiologically, this would have the effect of reducing the in vivo axial stretch of the artery as the constituents remodel about the new basal state.

The remodelling parameters are determined by first selecting a value of α that corresponds to a realistic turnover rate for the collagen fibres, and then choosing β such that dilation is physiologically realistic over a timescale of 10 years. The free variable is the remodelling of the collagen density. This must be examined to see if, once α and β have been prescribed, the remodelling of the density of fibres is physiologically consistent. Not surprisingly, the density remodels to the greatest extent in the central region of the aneurysm, which undergoes the greatest deformation. The adventitial collagen density remodels more than medial collagen—this may be attributed to the adventitial collagen being more axially orientated so it is subject to greater strains due to the high axial deformation in the central region of the aneurysm. The remodelling of the collagen density n_J in the medial and adventitial layers at first seems excessive, with maximum increases of 25 times in the media (Fig. 6a) and 30 times in the adventitia (Fig. 6b). However, n_J defines the collagen density with respect to the *undeformed* configuration of the tissue. The remodelled in vivo aneurysmal tissue may retract only slightly due to the loss of elastin and remodelling of constituents about the new basal state. In fact, Fukui et al. (2002) report mean axial and circumferential in vivo stretches of aneurysmal arterial tissue of 5 and 12% respectively. The in vivo physiological pre-stretch of the healthy abdominal aorta is 1.5, therefore the tissue must have remodelled about the deformed configuration. Thus, it may be more appropriate to define the collagen

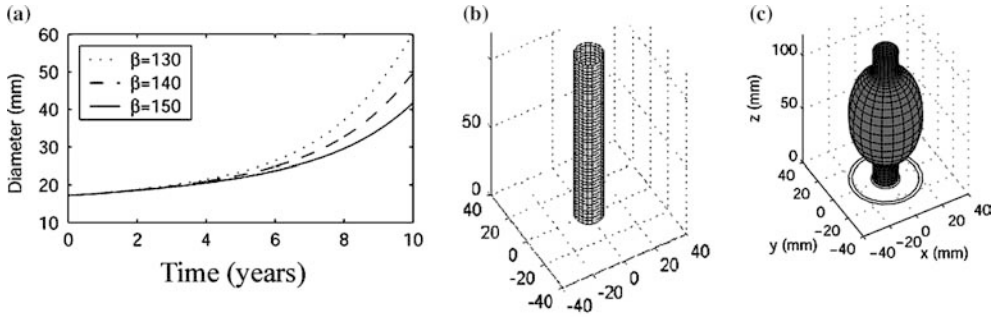

Fig. 5 **a** Plots of the maximum diameter of the axisymmetric aneurysm model vs. time showing that a physiologically realistic dilation is obtained for $\alpha = 12$ (corresponding to a half-life of 6 months) and $130 < \beta < 150$. This range of parameters gives physiologically realistic dilation, i.e. the aneurysm diameter increases by a factor of 2–3 over 10 years. **b** The initial undeformed geometry at $t = 0$. **c** The axisymmetric solution at 10 years using $\alpha = 12$, $\beta = 140$ ($m_1 = 20$, $m_2 = 0$). The Lagrangian mesh superimposed on the midplane of the aneurysm is attached to the material points and illustrates the deformation from the initial state

density with respect to the current deformed configuration, $\tilde{n}_J(x^1, t) = n_J(x^1, t)/|\mathbf{A}_1 \wedge \mathbf{A}_2|$, where $\mathbf{A}_1$ and $\mathbf{A}_2$ are the deformed midplane basis vectors. This gives increases in density of a factor of 2–3 (Fig. 6c and d).

The axisymmetric model may be employed to examine the effect that changes in the pressure have on the rate of remodelling. To simulate the onset of hypertension the pressure is increased stepwise after 2 years by factors of 1.1, 1.2 and 1.3. As expected, greater pressures give greater dilation rates (Fig. 7). Importantly, for a pressure change of up to 30%, the predicted dilations are still physiologically consistent, i.e. 0.3–1.1 cm per year (Humphrey 2002). These results have an obvious clinical application in that patients with aneurysms should have therapy to prevent hypertensive conditions.

9 Example of an asymmetric aneurysm

Asymmetric aneurysms can be developed either by assuming an asymmetric degradation of elastin or by assuming an axisymmetric degradation of elastin and postulating that the spine limits posterior expansion. The physiologically determined remodelling-rate parameters for the axisymmetric model ($\alpha = 12$, $\beta = 140$) are used in the subsequent analysis. Here the elastin is degraded axisymmetrically, and a penalty pressure approach is used to model spinal contact. The spine is modelled as a stiff spring-backed plate. Where the aneurysm wall penetrates the plate, a penalty pressure acts normal to the aneurysm. The effective pressure

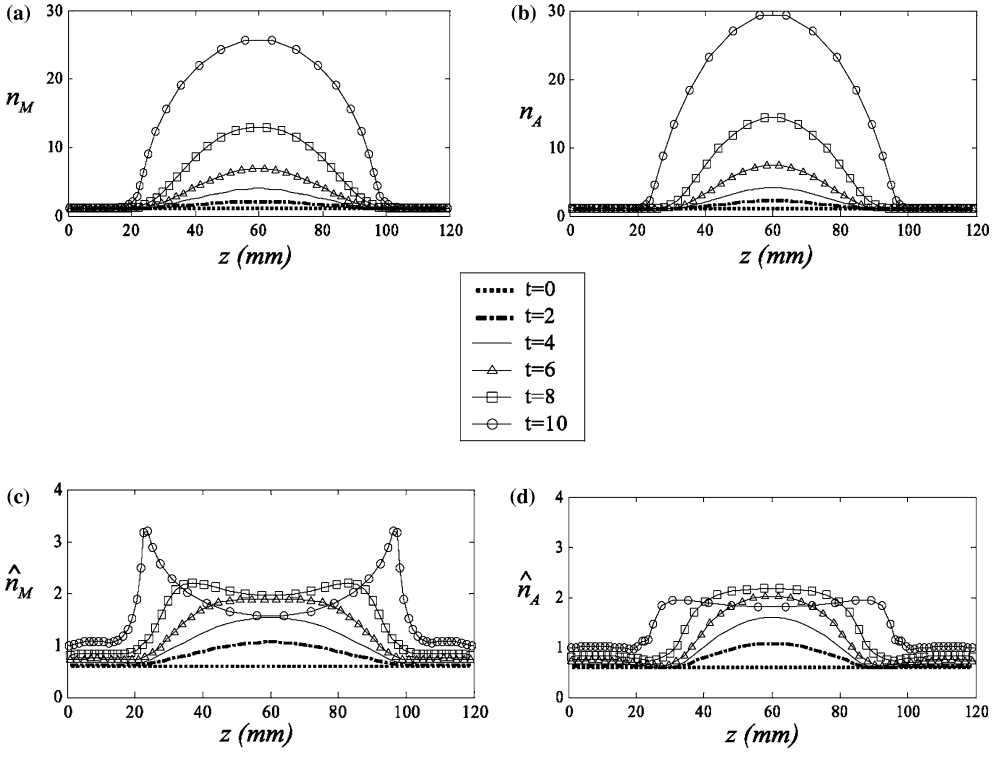

Fig. 6 Remodelling of the **a** medial n_M and **b** adventitial n_A, collagen density vs. Eulerian axial coordinate z for the axisymmetric model shown in Fig. 4b, t denotes time in years. The predicted results seem high. However, if one takes into account the distortion of the tissue in the altered configuration, more realistic results are obtained: remodelling of **c** medial $\hat{n}_{\mathrm{M}}$ and **d** adventitial $\hat{n}_{\mathrm{A}}$ collagen density with respect to the deformed configuration. Note that the rapid increase in dilation of the central region in later years results in a drop in density with respect to the deformed configuration in this region

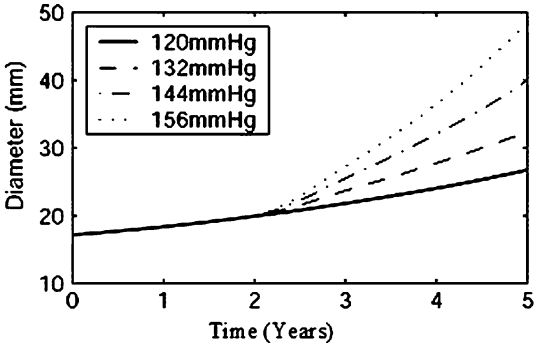

Fig. 7 The rate of dilation of the axisymmetric aneurysm increases in hypertensive conditions and is physiologically consistent. The remodelling parameters are fixed ($\alpha = 12$, $\beta = 140$) and the same degradation of elastin (Fig. 5a) is used for each case

acting on the membrane, $p(x^1, x^2, t)$ is given by the difference of internal physiological pressure and the penalty pressure. For further details, see Watton (2002). The contact with the spine results in a preferential anterior bulging in the aneurysm (Fig. 8a).

Axial and azimuthal Cauchy stresses, normalized with respect to the initial stresses in the healthy abdominal aorta at systolic pressure, are considered on the anterior and posterior wall. A rupture criterion based on the stresses on the tissue is not known—indeed, the use of such a criterion would be useful only if the stresses in an aneurysm in a living person could be accurately measured. Thus a criterion based on the diameter serves more usefully. However, mathematical models can easily define the stresses in the aneurysm, which may be useful in determining the shapes of aneurysm that are more likely to rupture. The Cauchy stresses relate to the stress that the tissue 'feels'; relative changes in the magnitude of stresses with respect to their normotensive levels may be a suitable indicator for likelihood of rupture. The purpose of our model is to show that a model for an aneurysm can be developed by considering it to be a consequence of changes to the tissues composition. To further test the validity of our model, the stresses it predicts will be compared with others predicted in the literature.

The stresses, averaged across the thickness of the arterial wall, will be considered on the anterior surfaces and posterior surfaces, along deformed coordinate lines, where $x^2 = 0$ and $x^2 = \pi R$. Due to the symmetry of the aneurysm along these deformed coordinate lines, there are no shear strains. Thus, the average Cauchy stress through the thickness of the wall is given by

$$t_{\mathrm{av}}^{11} = (2\varepsilon_{11} + 1)S_{\mathrm{av}}^{11}, \quad t_{\mathrm{av}}^{22} = (2\varepsilon_{22} + 1)S_{\mathrm{av}}^{22}, \tag{41}$$

where ${t_{\mathrm{av}}}^{11}$ and ${t_{\mathrm{av}}}^{22}$ denote the average Cauchy stresses in the direction of the deformed x^1 and x^2 coordinates. The quantities ${S_{\mathrm{av}}}^{11}$ and ${S_{\mathrm{av}}}^{22}$ are the average second Piola–Kirchhoff stresses. The media is twice the thickness of the adventitia and thus the average stress is weighted accordingly,

$$S_{\mathrm{av}}^{11} = \frac{\partial((2w_{\mathrm{M}} + w_{\mathrm{A}})/3)}{\partial\varepsilon_{11}}, \quad S_{\mathrm{av}}^{22} = \frac{\partial((2w_{\mathrm{M}} + w_{\mathrm{A}})/3)}{\partial\varepsilon_{22}}. \tag{42}$$

The stresses can be normalized with respect to axial and azimuthal stresses at the systolic pressure in the healthy abdominal aorta,

$$\hat{t}^{11} = \frac{t_{\mathrm{av}}^{11}}{t_{\mathrm{av}_0}^{11}}, \quad \hat{t}^{22} = \frac{t_{\mathrm{av}}^{22}}{t_{\mathrm{av}_0}^{22}}, \tag{43}$$

where $t_{\mathrm{av}_0}^{11}$ and $t_{\mathrm{av}_0}^{22}$ denote the average axial and azimuthal Cauchy stresses in the abdominal aorta at systole at $t = 0$. Plots of the normalized Cauchy stresses on the anterior and posterior wall are shown in Fig. 9. Stresses increase in the region of maximum dilation. The azimuthal stresses increase more than the axial stresses, and stresses are greater on the anterior wall than the posterior wall. At the proximal and distal ends of this aneurysm, the axial stresses have dropped almost to zero and there is a small reduction in the azimuthal stresses. The stress analysis agrees with the previous analysis (Elger et al. 1996) in that the azimuthal stresses increase more than the axial stresses. Also, the axial stress decreases towards the distal and proximal ends of the aneurysm. However, the model predicts increases in the Cauchy stresses that are particularly greater than in previous models, i.e. 10–18 times, whereas Elger et al. (1996) calculate increases by a factor of 2–3. This is a consequence of the axial strains in the central region of the aneurysm increasing to such an extent that, in the deformed configuration, a substantial thinning of the membrane has occurred (Fig. 8b). Thus, the Cauchy stresses, which define stresses with respect to deformed area elements, are very high.

In this work, collagen remodelling has been achieved by changing the collagen fibre density. However, deposition of collagen may arise by adding more tissue,

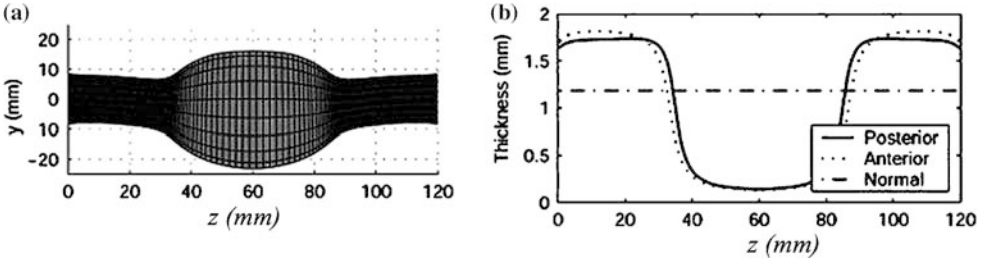

Fig. 8 Profile of an aneurysm using an axisymmetric degradation of elastin ($m_1 = 5$, $m_2 = 0.25$) and introducing contact at y = 15 mm. Spinal contact has resulted in preferential anterior bulging. **b** The deformed thickness of the aneurysm is very thin

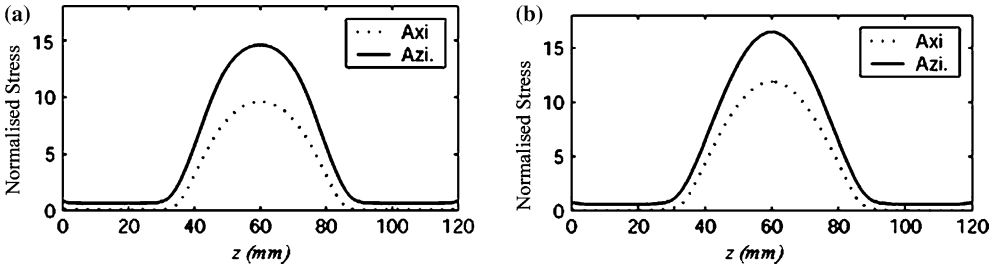

Fig. 9 Normalized Cauchy stresses in the asymmetric aneurysm with spinal contact at 10 years: **a** posterior, **b** anterior. Azimuthal stresses increase by a greater factor than the axial stresses. The magnitudes are high due to the substantial thinning of the membrane in the model

rather than increasing the density. Mathematically, the equilibrium deformation field is dependent on the strain energy stored inside the arterial wall. The deformation field for a thickening of the wall would be equivalent to that of an increase in density, provided that this represented the same number of fibres per unit area of the membrane, and the wall remained thin enough for the membrane approximation to be made. The density is the preferred variable to consider for remodelling purposes, since this relates to the mass of the collagen in the wall, whereas there is ambiguity in the microstructural interpretation of a remodelled thickness. Nevertheless, to correctly estimate stresses, it may be more appropriate if they are defined with respect to a physiologically realistic aneurysm wall thickness. Elger et al. (1996) considered the wall thickness of the aneurysm to be uniform in the deformed configuration. The stress distributions in this model can be examined by assuming that the wall thickness in the deformed configuration is constant.

The Cauchy stresses are defined with respect to the deformed arterial wall thickness h_{def}, i.e. $h_{\text{def}} = h/|\mathbf{A}_1 \wedge \mathbf{A}_2|$, where $h = h_{\text{M}} + h_{\text{A}}$ is the undeformed thickness, and $|\mathbf{A}_1 \wedge \mathbf{A}_2|$ is the determinant of the mid-plane metric tensor. Now consider the forces acting on a membrane element: if the thickness of the element increases by a factor f, then the stress must decrease by a factor f for the force to remain the same. The (virtual) factor by which the deformed aneurysm membrane must thicken to achieve a uniform systolic thickness is $f = |\mathbf{A}_1 \wedge \mathbf{A}_2|_{t=T}/|\mathbf{A}_1 \wedge \mathbf{A}_2|_{t=0}$; the initial systolic thickness for the healthy axisymmetric model of the abdominal aorta is $h_{\text{sys}} = h/|\mathbf{A}_1 \wedge \mathbf{A}_2|_{t=0}$. Thus the stresses (acting in the deformed configuration) defined with respect to an arterial wall of uniform systolic thickness, $\hat{t}^{\alpha\alpha}_{\text{unif}}$, are given by

$$\hat{t}^{\alpha\alpha}_{\text{unif}} = \frac{\hat{t}^{\alpha\alpha}|\mathbf{A}_1 \wedge \mathbf{A}_2|_{t=0}}{|\mathbf{A}_1 \wedge \mathbf{A}_2|_{t=T}} \quad \text{for } \alpha = 1,\ 2. \tag{44}$$

Plots of the stress distributions on the posterior and anterior walls, for an aneurysm wall of uniform systolic thickness, are shown in Fig. 10. The relative magnitudes and distributions of the stresses are now in agreement with Elger et al.'s (1996) findings. Furthermore, the distribution of the stress compares favourably with the stress analysis of an asymmetric aneurysm model used by Raghavan and Vorp (2000). They proposed an isotropic homogeneous SEDF for aneurysmal tissue and used an idealized asymmetric geometry for the aneurysm, with no attempt to model spinal contact. The von Mises stresses were found to be lower towards the proximal and distal ends, had peaks in the necks of the aneurysm, and had a local maximum stress that was located at the centre of the posterior wall. We obtained similar results with the exception that there is a local maximum azimuthal stress on the anterior wall and not the posterior wall (Fig. 10). However, this difference may be attributed to two differences in the modelling. Firstly, our model includes spinal contact, which would act to support the posterior wall and thus will reduce the stresses in this region. Secondly, the geometry of the asymmetric aneurysm differs. Raghavan and Vorp's (2000) aneurysm's geometry is more asymmetric, the anterior wall bulges substantially whilst there is negligible bulging of the posterior wall. We did find though, that if an asymmetric aneurysm is developed using an asymmetric degradation of elastin, with no spinal contact, then maximum azimuthal and axial stresses occurred on the center of the posterior wall (Watton 2002). An interesting and possibly important result is obtained when one examines the distribution of the axial stress. On the anterior wall it has a localized minimum close to the distal and proximal ends of the aneurysm. This may indicate a propensity for the aneurysm to buckle.

The model allows for the strain fields in the elastin and collagen to be examined independently. The strains in the collagen fibres are defined with respect to the deformed configuration by means of the recruitment

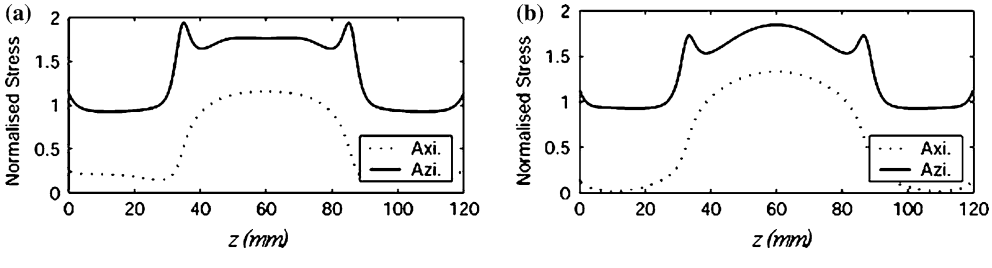

Fig. 10 Cauchy stresses ($t = 10$ years) for asymmetric aneurysm with constant wall thickness in deformed configuration **a** posterior, **b** anterior. This yields distributions and magnitudes in general qualitative agreement with previous studies

variables, whilst the strains in the elastin are defined with respect to the initial undeformed configuration of the artery. This may be an important feature if the eventual rupture of the aneurysm is attributed to the failure of a particular material. Figure 11a shows the distribution of the strains in the elastin and Fig. 11b the strains in the collagen fibres, on the anterior of the aneurysm. Similar results are found for the posterior wall although, as expected, the strains on this wall increase slightly less. The azimuthal strains in the elastin are highest in the central region of the aneurysm and close to normotensive values towards the distal and proximal ends of the abdominal aorta. The axial strains in the elastin peak in the central region of maximum dilation, and fall to zero towards the proximal and distal ends of the aorta. Collagen fibre strains are greatest in the central region of maximum dilation and have remodelled to normotensive values towards the distal and proximal ends of the abdominal aorta. The adventitial fibre strains increase to a greater extent than the medial fibre strains because the adventitial fibres are more axially orientated and the greatest deformation occurs in the axial direction. Overall strains in both the elastin and collagen increase to the greatest extent on the anterior wall at the point of maximum dilation. The small increase in collagen strains is a consequence of the remodelling of the recruitment variables and the fibres strains being defined with respect to an altered configuration. The much larger increase in the elastin strains are a result of the artery being subject to an initial axial pre-stretch which causes the central region of the artery to dilate and the distal and proximal ends to retract as the elastin degrades.

10 Conclusions and discussion

The model developed here is the first mathematical model to consider the evolution of the AAA. It uses a realistic structural model for the healthy abdominal aorta and implements the remodelling of the constituents using structural remodelling equations. However, this model does not explain why aneurysms are most likely to occur in the abdominal aorta and not elsewhere in the body. Furthermore, the central assumption that drives the remodelling, the degradation of elastin, is assumed and prescribed. No attempt is made to model the cause of the loss of elastin, nor to explain why this primarily occurs in the abdominal aorta. These are important matters, which require increased physiological knowledge; new mathematical models may guide research. However, there are more immediate criticisms of the model that could be addressed in subsequent work.

During development of the aneurysm, the Green's strains in the elastin become very large. The isotropic neo-Hookean SEDF used to model the elastin's mechanical behaviour may not be valid at such large strains; an alternative SEDF may be required. However, it is likely that some creeping of the elastinous tissue occurs. To model such a process would require that the elastin strains are defined with respect to a deformed configuration, in which case the isotropic neo-Hookean SEDF (defined with respect to the strains in an altered configuration) may be valid. Also, the ground substance may creep. This is probably not significant in our calculations because it bears only a small proportion of the total load, yet it is probably able to resist a compressive load and could lead to in vivo aneurysms not retracting fully to the undeformed state.

The spatial degradation of elastin may have been unrealistic. The Lagrangian function, which is used to model the degradation, deforms with the material coordinates. Thus, due to the distortion of the tissue in the central region of the aneurysm, the relative concentration of elastin would be of the order of $10\%/((\mathbf{A}_1 \wedge \mathbf{A}_2)|_{t=T} \approx 1\%$. This is approximately an order lower than the lowest experimental estimates, i.e. 8% (He and Roach 1993). The substantial axial distortion of the aneurysm is a consequence of degrading the elastin in the central region whilst assuming it does not degrade towards the distal and proximal ends. The concentration difference causes the axial dilation of the central region and retraction of the ends. If the elastin were degraded uniformly along the length of the artery, then such high axial distortions would not occur. This may account for the unrealistic thinning of the membrane that is predicted by the model. Further experimental work is necessary to accurately determine spatial distributions in developed aneurysms to improve the mathematical model.

It has been assumed that the collagen fibre angles deform with the tissue as the aneurysm deforms; this is

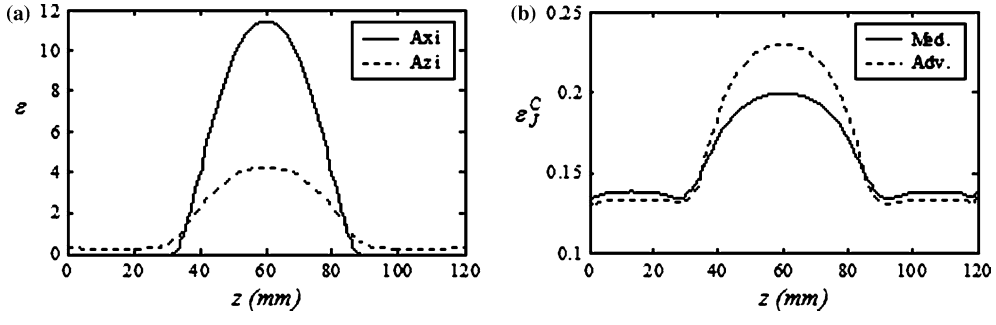

Fig. 11 Green's strains on anterior wall of aneurysm at $t = 10$ years for **a** elastin **b** collagen fibres. Note that the strains in the elastin increase substantially since they are defined with respect to the undeformed configuration of the tissue, whereas collagen fibre strains are much lower due to the remodelling

questionable. The structural arrangement of fibre angles in the healthy abdominal aorta is known, but the structure in an aneurysm is not. It is likely that the fibres distribute themselves so that the tissue behaves in an optimum manner. If a physiological/mechanical criterion for fibre alignment were known, then the fibre angles could be treated as free variables and allowed to remodel. Indeed if the fibre angles in diseased tissue were known, remodelling hypotheses for fibre alignment could be tested with this model.

The remodelling equations for the recruitment and fibre density variables have been given simple linear forms and the remodelling parameters, α and β, have been assumed to take the same values in the media and adventitia. It is questionable as to whether a linear function realistically represents the remodelling behaviour and whether the remodelling rate parameters for the media should be equal to those for the adventitia. For example, if turnover rates and increased rates of deposition are affected by cellular activity, then, since elastin degradation occurs in media, the remodelling rates should be higher in the media. In vivo, aneurysms are reported to have an appreciably thicker adventitia than media (Humphrey 2002). A suitably sensitive, nonlinear remodelling function could allow for greater increases in the adventitia and less in the media, or the value of the remodelling parameter β could be increased for the adventitia and decreased for the media. However, such modelling is phenomenological and does not yield an insight into the underlying physical mechanisms causing the increased deposition in the adventitia. An alternative approach, that may be more appropriate, would be to use a remodelling equation for the thickness of the arterial wall that acts to maintain an equilibrium stress. However, this would not yield information about changes in the structural composition. Although this model does not accurately predict thicknesses of the arterial wall it does predict how much mass of collagen there will be in the developed aneurysm wall, which could be measured experimentally. Further experimental investigation is needed to assist in determining the most appropriate form the remodelling functions should take.

The abdominal aorta has been modelled as a perfectly cylindrical tube. In fact, there is a small degree of tapering and a small amount of tortuosity; an axial section of abdominal aorta of length 11.0 cm has an actual straight length of 11.5 cm (Raghavan and Vorp 2000). It was seen in this work that the axial stress could fall to a minimum of zero, close to the neck of the aneurysm. The reduction in axial stress (that occurs as the elastin is lost and the collagen remodels) coupled with an initial asymmetric geometry may predict the highly tortuous aneurysms often seen in vivo.

The remodelling hypothesis assumes that the fibres attach and configure to achieve a peak attachment strain. It was assumed that the peak strains in the fibres occur at systolic pressure. Thus, fibre attachment can be modelled by considering the steady deformations that occur as the constituents remodel at systolic pressure. However, for a more complex geometry, the fibres may not achieve maximum strains at systolic pressure. For example, towards the distal and proximal ends of the aneurysm the strains may increase as the pressure is reduced. The remodelling of fibres should be dependent on the peak strains of the fibres during the cardiac cycle. The remodelling assumption should thus be generalized so that no remodelling occurs if the peak strain in the fibre is equal to ε_A during the cardiac cycle, i.e.

$$\frac{dr_{J_p}}{dt} = \alpha\left(\varepsilon^C_{J_p}\Big|_{\max} - \varepsilon_a\right) \tag{45}$$

where $\varepsilon^C_{J_p}\Big|_{\max}$ is the maximum strain that occurs in the collagen during the cardiac cycle (diastolic to systolic). This would increase computational cost but would be relatively easy to include. Physically this would act to reduce the rate of remodelling towards the distal and proximal ends of the aorta.

The model does not include other physical features that would act to bear the load and limit the rate of dilation, such as the calcification of the wall or the intraluminal thrombus (Di Martino et al. 1998; Wang et al. 2001). Moreover, the effective transmural pressure would reduce as the aneurysm comes into contact with the surrounding tissue which would reduce the rate of dilation. Modelling of such features may be incorporated in future developments of the model.

All of the criticisms discussed so far could be addressed. However, one criticism is integral to the model. Increased deposition of collagen has been achieved by remodelling the fibre density within the tissue. The model does not predict by how much the wall will thicken. Consequently, the precise stress distributions in the aneurysm wall are unknown and some assumption regarding the remodelled thickness of the aneurysm is required.

Despite its shortcomings, our model yields results that are consistent with those observed in vivo and predicted by other mathematical analyses of developed aneurysms. Where possible we have based parameter values on those from the literature; however some of the estimates are coarse and further experimental research is required to accurately determine values. We believe this model may provide a theoretical basis for further experimentation and validation in the field.

Acknowledgements P. N. Watton gratefully acknowledges the award of a Research Studentship funded by the UK Medical Research Council. The authors are indebted to the Consultant Vascular Surgeons, Mr S. Dodds (Good Hope Hospital, Sutton Coldfield, UK) and Mr D.A.J. Scott (St. James's University Hospital, Leeds, UK) for many helpful discussions about the clinical aspects and physiology of abdominal aortic aneurysms. We also acknowledge the Harwell Software Library (http://www.hsl.ac.uk) for granting UK academics the free use of its Fortran subroutines in non-commercial applications. MA38 was employed to solve the linear system that arises in the Newton iteration, which is required to update the deformation at successive timesteps.

References

Alberts B, Bray D, Lewis J, Raff M, Roberts K, Watson JD (1994) Molecular biology of the cell, 3rd edn. Garland Publishing, New York

Armeniades CD, Lake LW, Missirlis YF (1973) Histological origin of aortic tissue mechanics: the role of collagenous and elastic structures. Appl Polym Symp 22:319–339

Armentano R, Levenson J, Barra J, Fischer E, Breitbart G, Pichel R, Simon A (1991) Assessment of elastin and collagen contribution to aortic elasticity in conscious dogs. Amer J Physiol 60:H1870–H1877

Cheng CP, Parker D, Taylor CA (2002) Quantification of wall shear stress in large blood vessels using lagrangian interpolation functions with cine phase-contrast magnetic resonance imaging. Ann Biomed Eng 30:1020–1032

Di Martino E, Mantero S, Inzoli F, Melissano G, Astoe D, Chiesa R, Fumero R (1998) Biomech. of abdominal aortic aneurysm in the presence of endoluminal thrombus: experimental characterisation and structural static computational analysis. Eur J Vasc Endovasc Surg 15:290–299

Elger D, Blackketter D, Budwig R, Johansen K (1996) The influence of shape on the stresses in model abdominal aortic aneurysms. J Biomech Eng 118:326–332

Fukui T, Matsumoto T, Tanaka T, Ohashi T, Kumagai K, Akimoto H, Tabayashi K, Sato M (2002) Biaxial tensile properties of aortic aneurysm tissues under equibiaxial stress. In: Proceedings of the world congress of biomechanics, Calgary, Alberta

Fung YC, Choung CJ (1986) On residual stresses in arteries. J Biomech 108:189–192

Fung YC, Liu SQ, Zhou JB (1993) Remodelling of the constitutive equation while a blood vessel remodels itself under stress. J Biomech Eng 115:453–459

He CM, Roach M (1993) The composition and mechanical properties of abdominal aortic aneurysms. J Vasc Surg 20(1):6–13

Heil M (1996) The stability of cylindrical shells conveying viscous flow. J Fluids Struct 10:173–196

Holzapfel GA (2000) Nonlinear solid mechanics. A continuum approach for engineering. Wiley, Chicester

Holzapfel GA, Gasser TC, Ogden RW (2000) A new constitutive framework for arterial wall mechanics and a comparative study of material models. J Elasticity 61:1–48

Humphrey JD (1995) Mechanics of the arterial wall: review and directions. Crit Rev Biomed Eng 23:1–162

Humphrey JD (1999) Remodelling of a collagenous tissue at fixed lengths. J Biomech Eng 121:591–597

Humphrey JD (2002) Cardivascular solid mechanics. Springer, Berlin Heidelberg New York

Lanne T, Sonesson B, Bergqvist D, Bengtsson H, Gustafsson D (1992) Diameter and Compliance in the male human abdominal aorta: influence of age and aortic aneurysm. Eur J Vasc Surg 6:178–184

Lever MJ (1995) Mass transport through the walls of arteries and veins. Biological flows. In: Jaffrin MY, Caro CG (eds) Plenum Press, New York, pp 177–197

MacSweeney S, Young G, Greenhalgh R, Powell J (1992) Mechanical properties of the aneurysmal aorta. Brit J Surg 79:1281–1284

Rachev A, Meister J (1998) A model for geometric and mechanical adaption of arteries to sustained hypertension. J Biomech Eng 120:9–17

Raghavan ML, Vorp DA (2000) Toward a biomechanical tool to evaluate rupture potential of abdominal aortic aneurysm: identification of a finite strain constitutive model and evaluation of its applicability. J Biomech 33:475–482

Raghavan ML, Webster M, Vorp DA (1999) Ex-vivo biomechanical behavior of AAA: assessment using a new mathematical model. Ann Biomed Eng 24:573–582

Rodriguez EK, Hoge A, McCulloch AD (1994) Stress-dependent finite growth in soft biological tissues. J Biomech 27:455–467

Shadwick R (1999) Mechanical design in arteries. J Exp Biol 202:3305–3313

Wang DHJ, Makaroun M, Webster MW, Vorp DA (2001) Mechanical properties and microstructure of intraluminal thrombus from abdominal aortic aneurysm. J Biomech Eng 123:536–539

Watton PN (2002) Mathematical modelling of the abdominal aortic aneurysm. PhD thesis, Department of Applied Mathematics, University of Leeds

Wempner G (1973) Mechanics of solids. McGraw-Hill, New York

Wilmink WBM, Quick CRG, Hubbard CS, Day NE (1999) The influence of screening on the incidence of ruptured abdominal aortic aneurysms. J Vasc Surg 30(2):203–208